SUPPLEMENTARY INFORMATION

Probing solid-state battery aging: evaluating calendar vs. cycle aging protocols *via* time-resolved electrochemical impedance spectroscopy

Thao Kim Truong[a], Grace Whang[a], Jake Huang[a], Stephanie Elizabeth Sandoval[a], Wolfgang G. Zeier[ab]*

[a]*Institute of Inorganic and Analytical Chemistry, University of Münster, 48149 Münster, Germany*

[b]*Institute of Energy Materials and Devices (IMD), IMD-4: Helmholtz-Institut Münster, Forschungszentrum Jülich, 48149 Münster, Germany.*

*Corresponding author email: wzeier@uni-muenster.de

Experimental

All sample preparation and cell assembly experiments were performed under argon atmosphere.

Li_6PS_5Cl synthesis

Li_6PS_5Cl solid electrolyte was synthesized via a solid-state synthesis method previously reported by our group[1]. Briefly, a stoichiometric mixture of Li_2S, P_2S_5, and LiCl was hand ground, pressed into pellets, and transferred into a carbon-coated quartz ampoule (12 mm inner diameter), which was then sealed under vacuum. The sample was annealed at 550 °C for 2 weeks. The resulting pellets were manually ground again to obtain the as-synthesized solid electrolyte powder.

Cathode composite preparation

The cathode composite was prepared by mild milling of the mixture of cathode active material $LiNi_{0.83}Co_{0.11}Mn_{0.06}O_2$ (NCM83, supplied by MSE) and the as-synthesized solid electrolyte Li_6PS_5Cl with a weight ratio of NCM83:Li_6PS_5Cl = 7:3. This was carried out via an “egg shape” vibratory ball mill (FRITSCH P-23) at 20 Hz for 15 min with 10 ZrO_2 grinding balls (Ø = 3 mm) per 100 mg batch of sample.

Cell assembly

The half-cell configuration In/InLi│Li_6PS_5Cl│NCM83:Li_6PS_5Cl was assembled in an airtight press cell housing with stainless steel current collectors[2] (Ø = 1 cm)[2]. First, 70 mg of the solid electrolyte Li_6PS_5Cl, serving as a separator, was first filled into the PEEK cylinder of the press cell and hand pressed. Then, 10 mg of the cathode composite (corresponding to an areal capacity of 1.783 mAh cm^{-2} based on NCM83 theoretical specific capacity of 200 mAh g^{-1}) was distributed on one side of the separator and a uniaxial pressure of 3 tons was applied for 3 min. Next, 51.2 mg of In/InLi alloy (≈28.42 at% Li, prepared from 50 mg In foil (9 mm in diameter, chemPUR, 99.999%) and 1.2 mg Li (cut from a Li rod (abcr, 99.8%) and subsequently pressed into a thin foil) was added to the other side of the separator such that the In foil was in contact with the solid electrolyte while the Li foil was in contact with the current collector. Finally, the press cell was closed and fixed in an aluminum frame, with a torque of 10 Nm providing an operating stack pressure of ~50 MPa. Cells were left at 25 °C for 6 h for equilibration before measurements.

Electrochemical testing

All electrochemical experiments were performed at 25 °C in a Binder climate chamber using a BioLogic VMP-300 potentiostat. In/InLi|Li_6PS_5Cl|NCM83:Li_6PS_5Cl half-cell configuration was used, with In/InLi anode serving as a counter electrode. The theoretical specific capacity of NCM83 used in this work was assumed to be 200 mAh g^{-1} as basis of calculation for charge and discharge current. Potentiostatic electrochemical impedance spectroscopy (EIS) was performed by applying an AC excitation with 10 mV root-mean-square amplitude superimposed to the open-circuit voltage (OCV) in a frequency range of 7 MHz–50 mHz. The measured impedance is defined as $Z(\omega) = Z_{Re} + jZ_{Im}$, where Z_{Re} and Z_{Im} are the real and imaginary parts of the complex impedance, respectively. The fitting of the data was implemented using DRT analysis. In DRT calculation, the impedance is modeled via an infinite Voigt circuit characterized by a distribution function $\gamma(\ln \tau)$ over relaxation times τ. The fundamental relation between the impedance and the DRT is expressed as[3]:

$$Z(\omega) = \int_0^\infty \frac{\gamma(ln\,\tau)}{1+j\omega\tau} d\,\tau \qquad (1)$$

In this report, the DRT was calculated (i.e. Eq. 1 was solved) for experimental EIS data. To obtain robust estimates of the DRT, we apply the self-tuning DRT inversion algorithm implemented in the python package hybrid-drt by Huang *et al*.[4] This uses a hierarchical Bayesian model to obtain the maximum *a posteriori* estimates of the DRT without manual parameter tuning, thereby ensuring consistent results. Since the impedance over the entire measured frequency range (7 MHz–50 mHz Hz) was found to obey the Kramers-Kronig relations, no frequencies were truncated prior to DRT inversion. The τ basis range used for the DRT was extended by 1 decade beyond the measured frequency bounds to prevent boundary artifacts due to truncation.

The protocol for aging tests was composed of three main steps: formation, accelerated aging, and reference performance test (RPT). In formation and RPT stages, cells were cycled three times at 0.1C rate between 2.0 and 3.7 V vs In/InLi. For the accelerated calendar aging experiments, cells were charged up to a cut-off with a constant current (CC) mode at 0.1C, followed by a constant voltage mode for 48 h before being discharged by another CC mode at 0.1C. For cycle aging experiments, charge-discharge cycles at 1C rate were conducted for approximately 48 h (actual durations varied slightly due to variations in cycle duration). For the cycling test, the lower cut-off of all cells was fixed at 2 V. EIS measurements were implemented every one hour during the potentiostatic hold, and at the end of discharge every two cycles during 1C cycling. For formation and RPT steps, EIS was measured at the

end of discharge of every cycle. It should be noted that before impedance measurement for formation, RPT, and 1C cycling periods, cells were rested at OCV for 30 minutes to ensure a pseudo-steady state. The upper cut-off potentials investigated for the aging period were 3.7, 3.8, 3.9, 4.0, and 4.1 V, which is hereafter simply referred to as cut-off in this report, since the lower cut-off was fixed for all cells as specified earlier. The employed accelerated aging protocols are schematically illustrated in **Figure 1** of the main text.

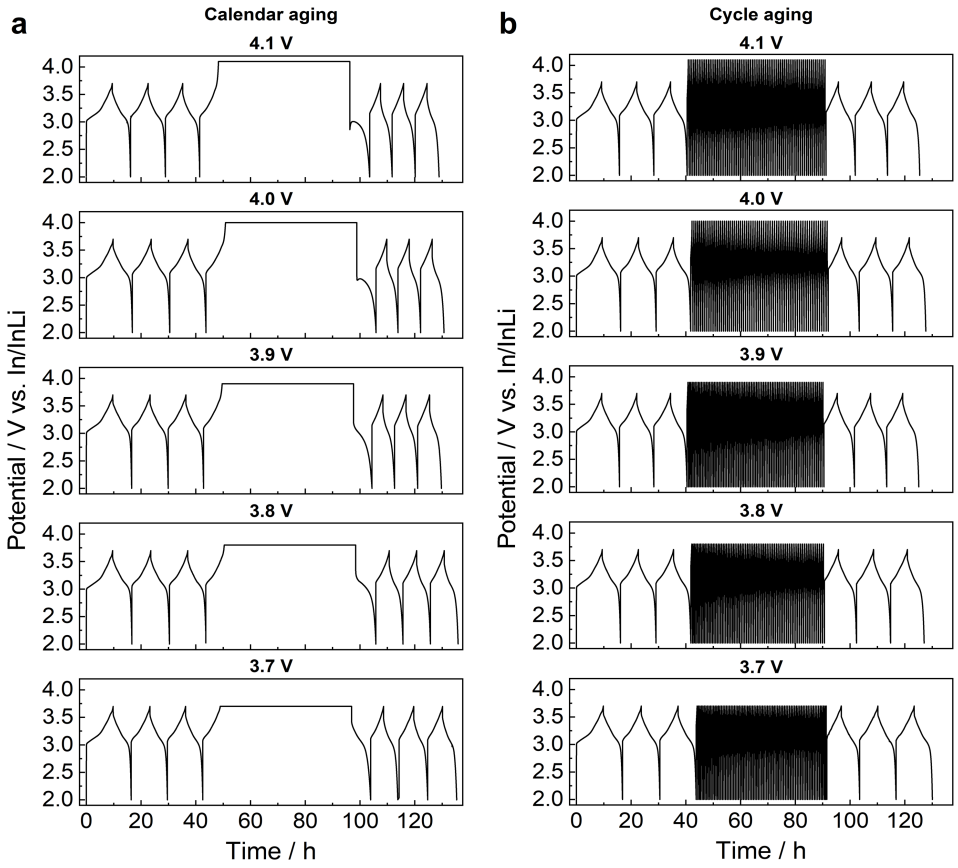

Figure S1. *Voltage versus time profile of accelerated (a) calendar aging and (b) cycle aging cells at different cut-offs.*

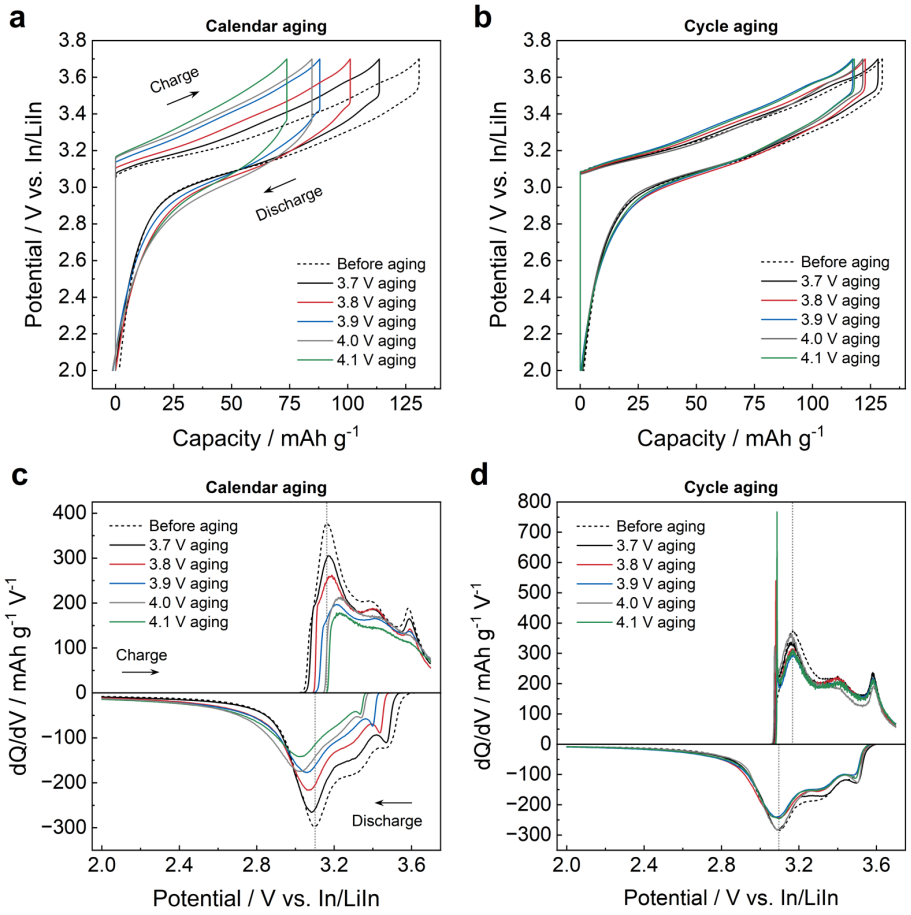

Figure S2. *Data measured in the last formation cycles (before aging) and last RPT cycles (aging). (a–b) Voltage versus capacity profiles and (c–d) corresponding differential capacity plots of accelerated calendar and cycle aging cells, respectively.*

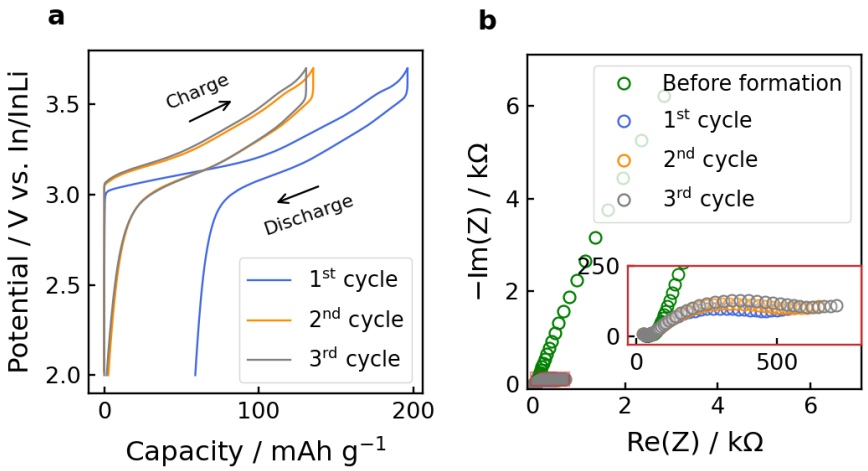

Figure S3. *Data recorded during formation step: (a) Representative potential versus capacity profiles and (b) Nyquist plots of the cell before formation and at the end of each discharge cycle.*

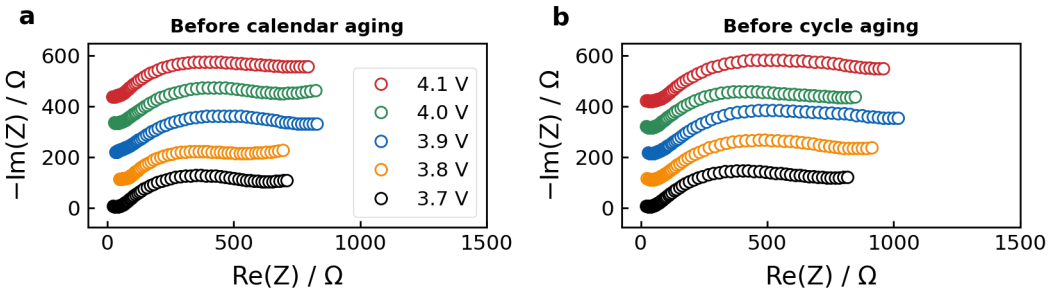

Figure S4. *Nyquist plots of the cells used for aging experiments after formation step.*

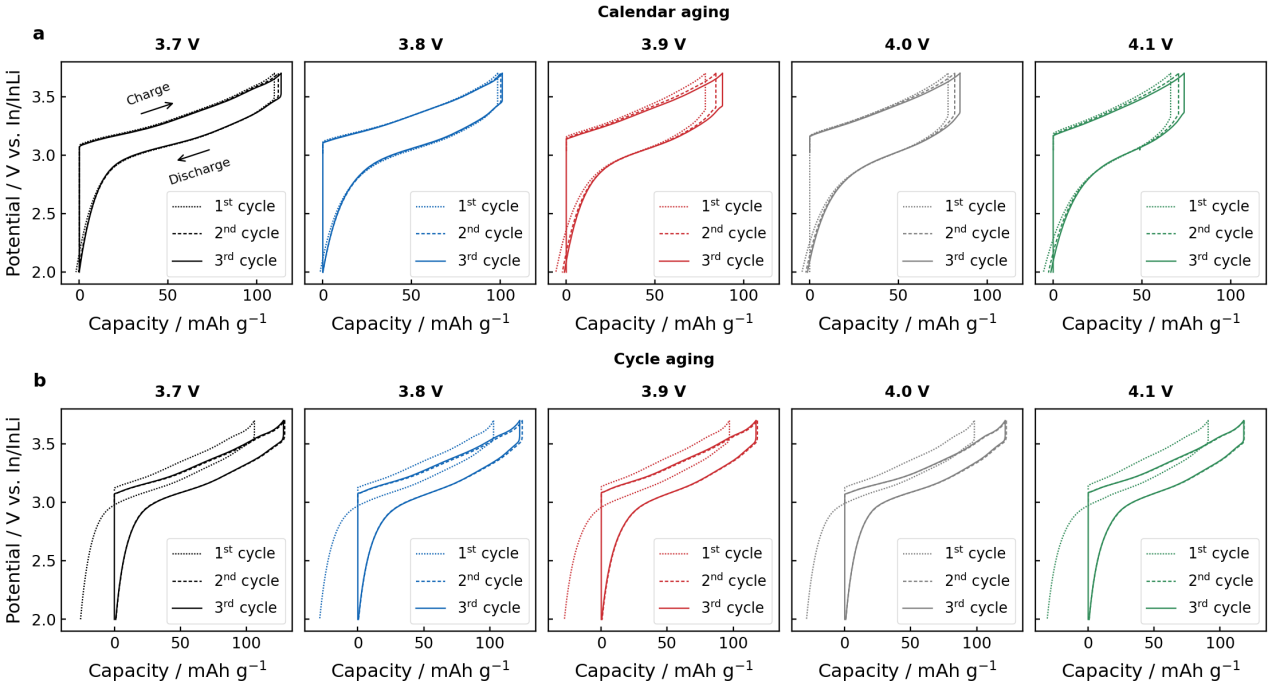

Figure S5. *Voltage versus capacity profiles of RPT cycles for (a) calendar aging and (b) cycle aging cells.*

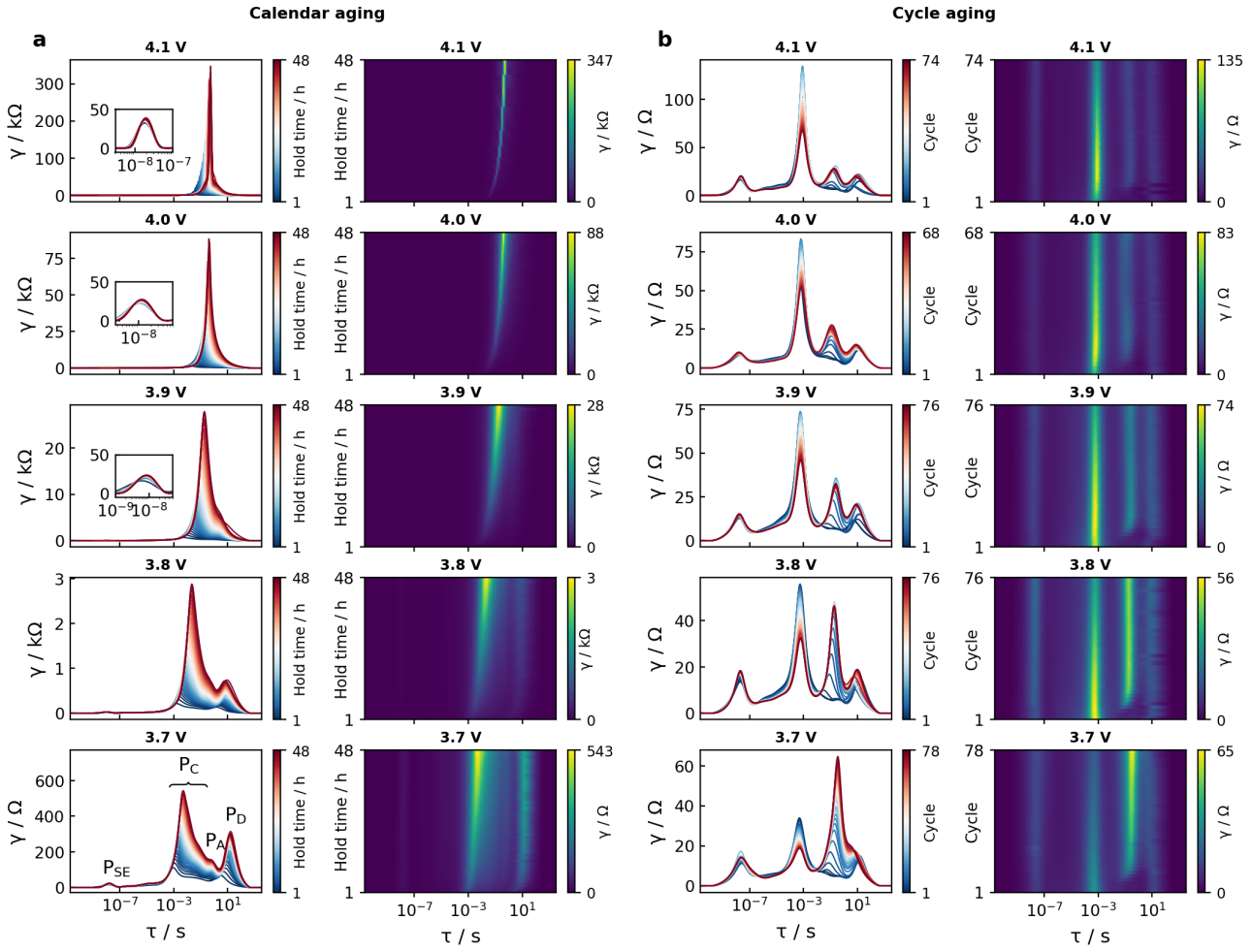

Figure S6. *DRT evolution and corresponding 2D DRT surfaces (a) during potentiostatic hold and (b) at end of discharge of cycles in high C-rate regime. In 2D DRT, the maximum value displayed on each color bar represents approximately the highest DRT intensity.*

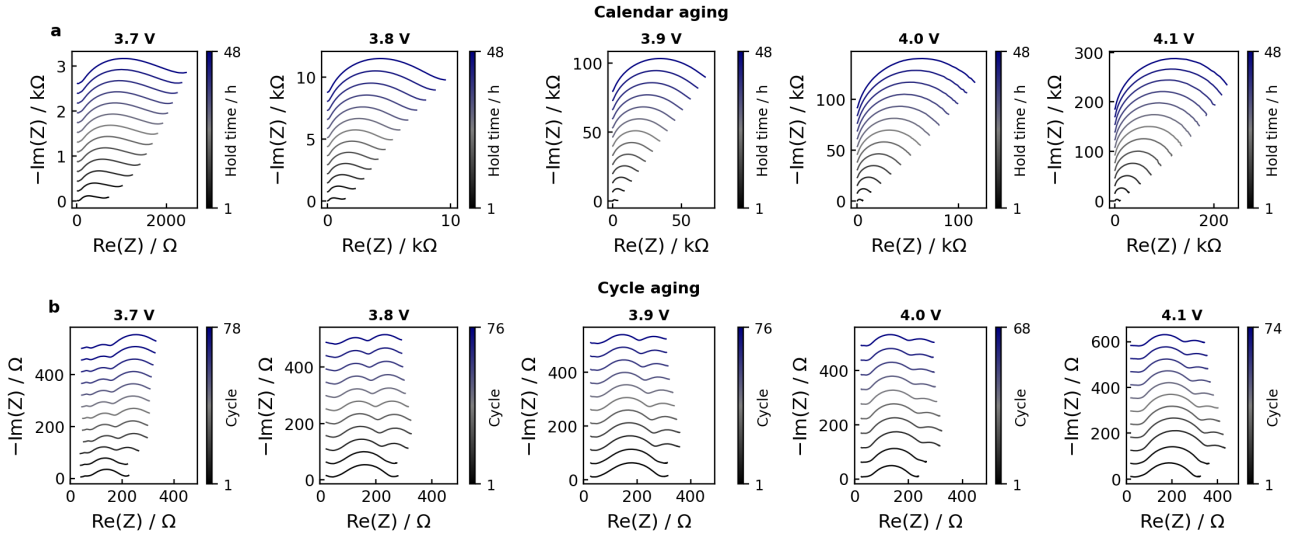

Figure S7. *Nyquist plots of (a) calendar aging and (b) cycle aging periods. Data are stacked at arbitrary constant offsets.*

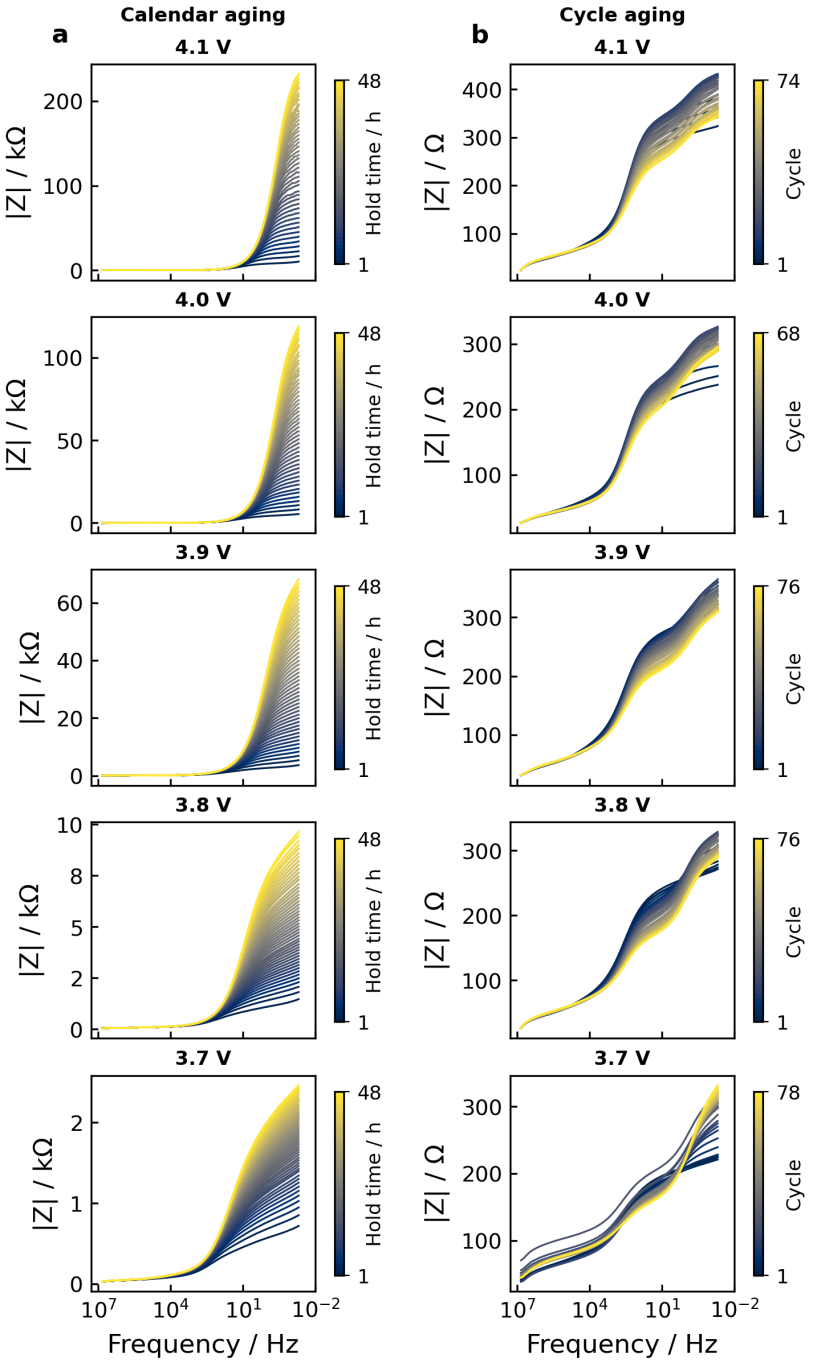

Figure S8. *Bode magnitude plots of (a) calendar aging and (b) cycle aging periods.*

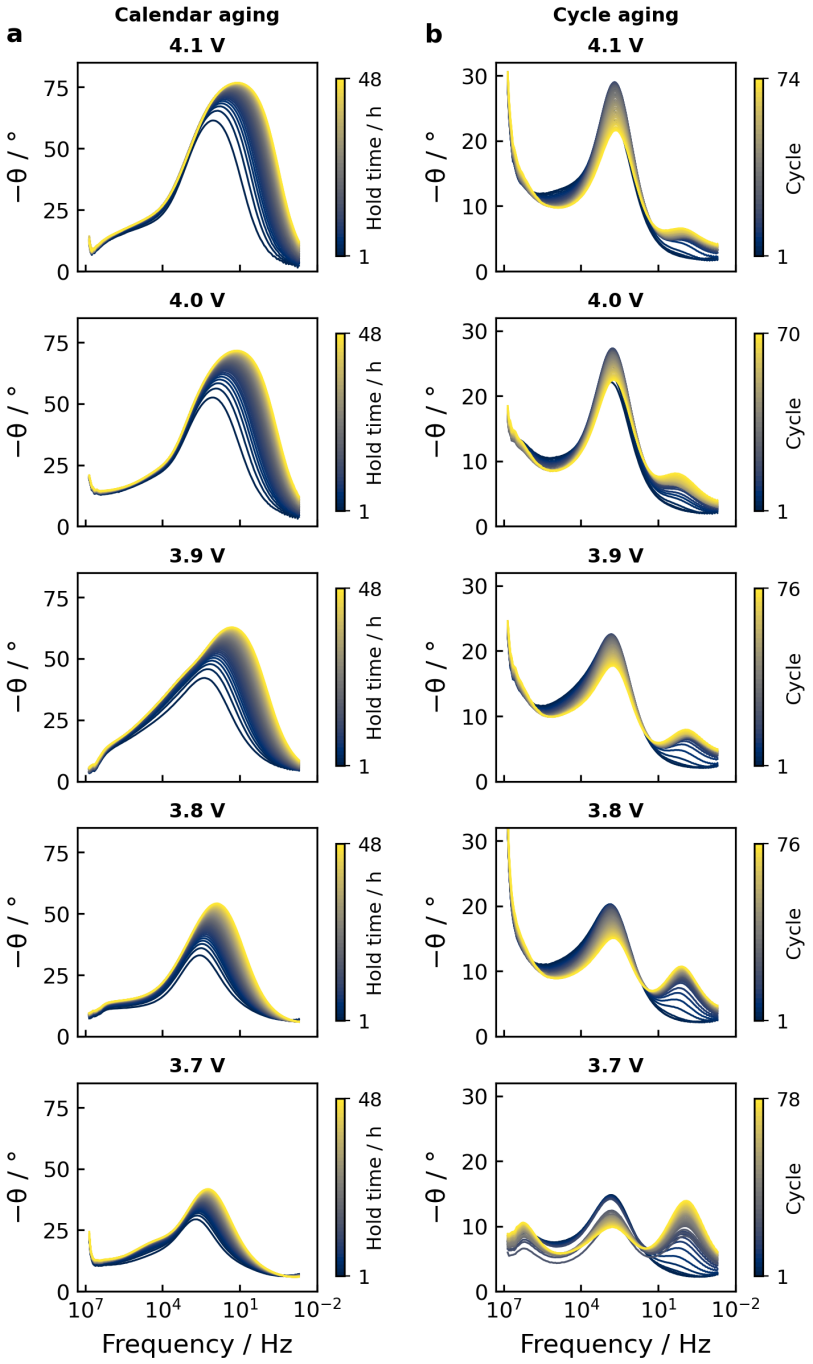

Figure S9. *Bode phase plots during (a) calendar aging and (b) cycle aging periods.*

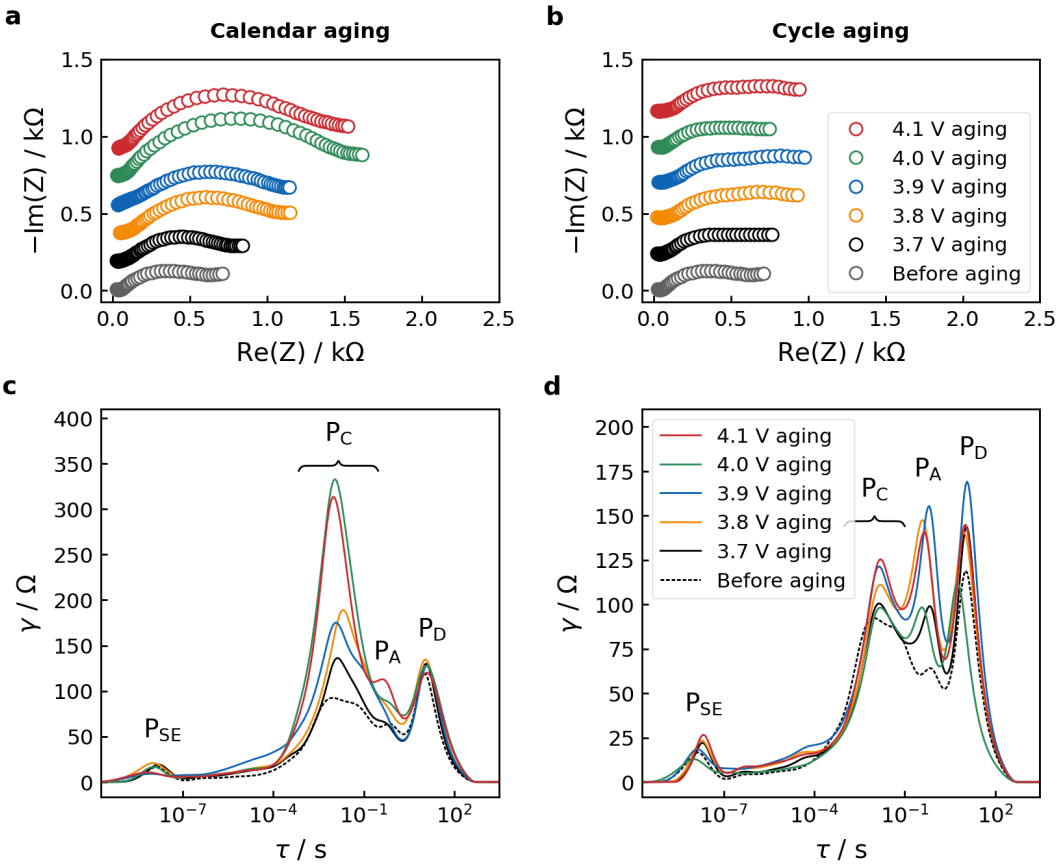

Figure S10. *Data measured at the last formation cycles (before aging) and last RPT cycles (aging). (a-b) Nyquist plots and (c-d) DRT of calendar and cycle aging cells, respectively.*

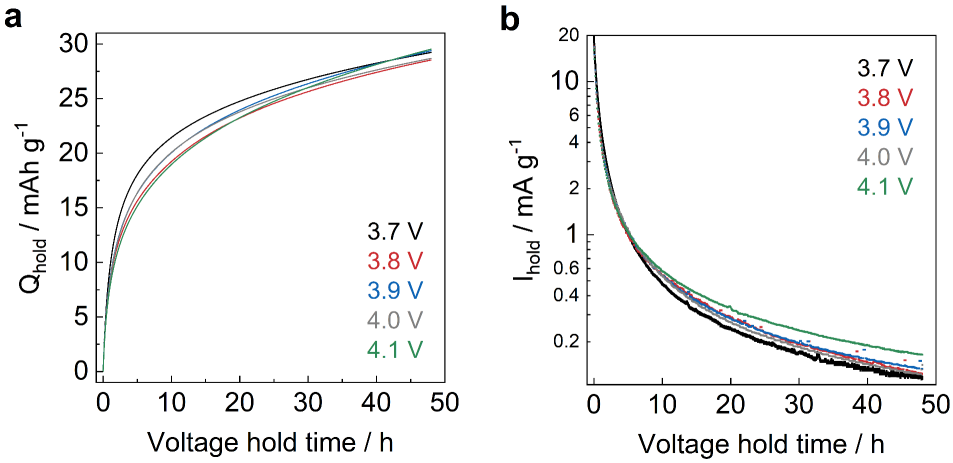

Figure S11*. (a) Capacity and (b) corresponding current versus time curves in potentiostatic hold periods.*

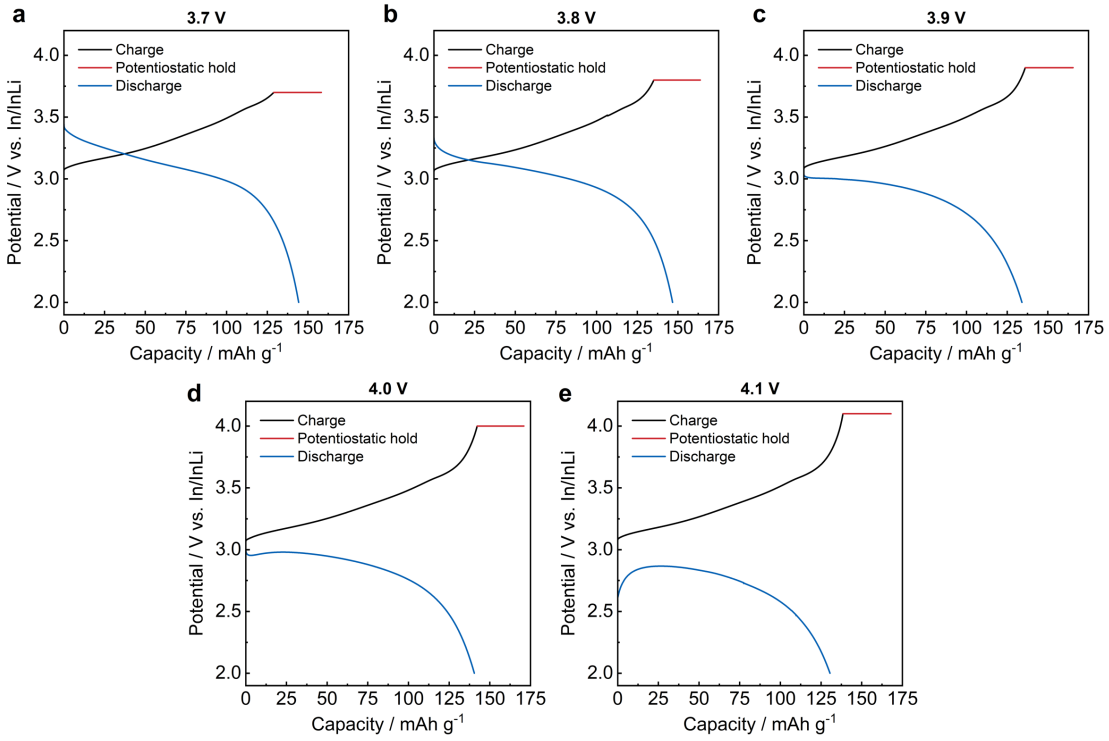

***Figure S12**. Galvanostatic charge-discharge curves of accelerated calendar aging cycles.*

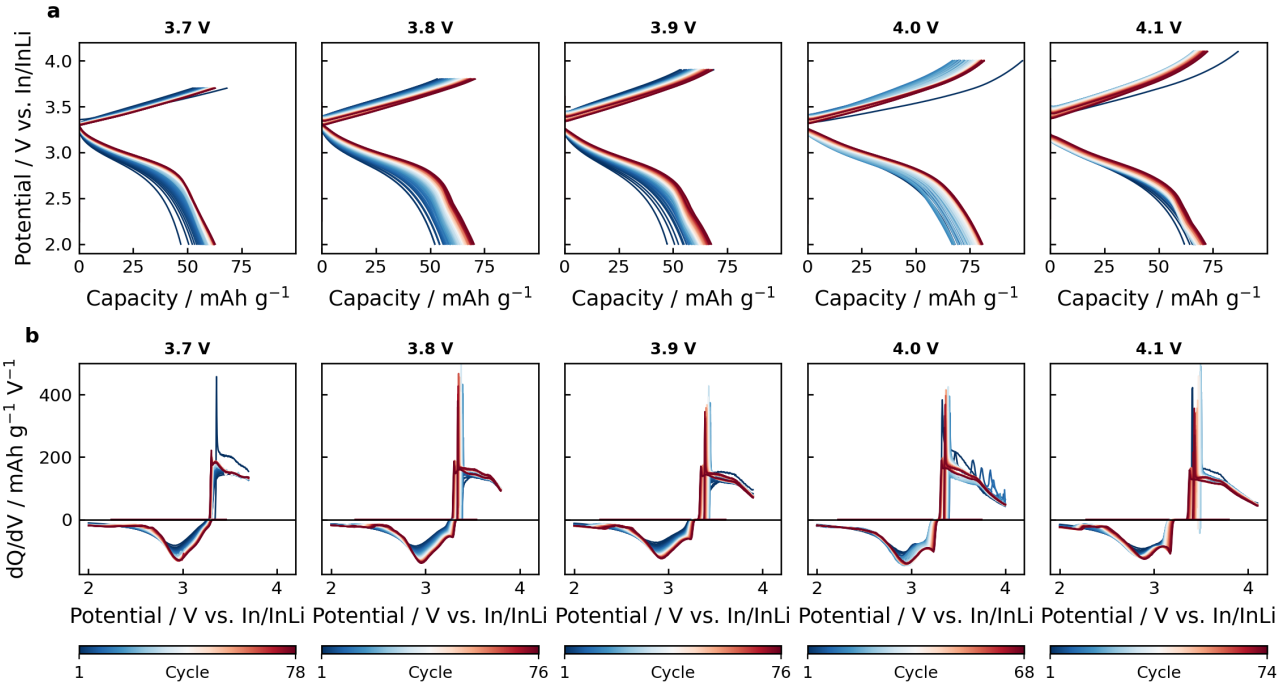

***Figure S13.** (a) Galvanostatic charge-discharge curves and (b) corresponding dQ/dV plots of cycle aging periods.*

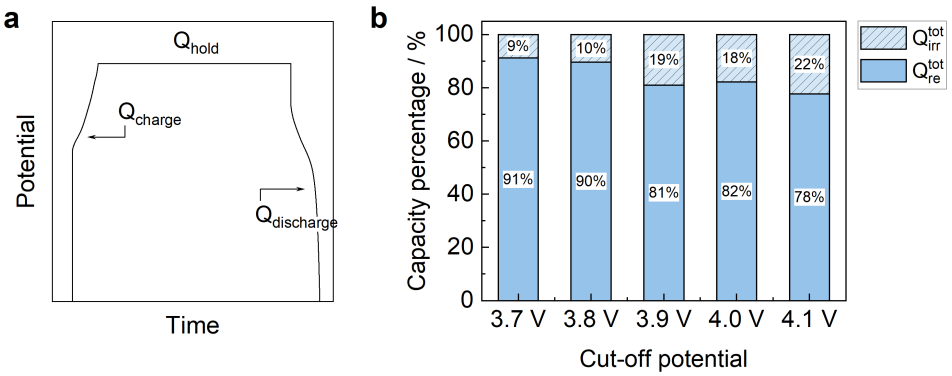

***Figure S14**. (a) Illustration of a typical cell voltage profile during calendar aging; (b) data calculated from **Figure S12**: total reversible (Q_{re}^{tot}) and total irreversible (Q_{irr}^{tot}) capacity contribution of accelerated calendar aging cycle at different cut-off potentials, with $Q_{re}^{tot} = Q_{discharge}$ and $Q_{irr}^{tot} = Q_{charge} + Q_{hold} - Q_{re}^{tot}$.*

References

1 M. A. Kraft, S. P. Culver, M. Calderon, F. Böcher, T. Krauskopf, A. Senyshyn, C. Dietrich, A. Zevalkink, J. Janek and W. G. Zeier, *Journal of the American Chemical Society*, 2017, **139**, 10909–10918.

2 T. T. Zuo, R. Rueß, R. Pan, F. Walther, M. Rohnke, S. Hori, R. Kanno, D. Schröder and J. Janek, *Nature Communications*, DOI:10.1038/s41467-021-26895-4.

3 K. Pan, F. Zou, M. Canova, Y. Zhu and J.-H. Kim, *Journal of Power Sources*, 2020, **479**, 229083.

4 J. Huang, N. P. Sullivan, A. Zakutayev and R. O'Hayre, *Electrochimica Acta*, 2023, **443**, 141879.